Supplementary Information (SI) for Physical Chemistry Chemical Physics.
This journal is © the Owner Societies 2024

Supplementary Information

Static disorder in perovskite-type proton-conducting oxides $BaSn_{1-x}M_xO_{3-x/2}$-$(y/2)H_2O$ (M = Ga, Sc, In, Y, La): A novel approach based on statistical analysis of numerous DFT simulated structures

Takanori Nagasaki*[a] and Tomoaki Yamada[a]

[a] *Department of Energy Engineering, Graduate School of Engineering, Nagoya University, Furo-cho, Chikusa-ku, Nagoya 464-8603, Japan. E-mail:* nagasaki.takanori.p4@a.mail.nagoya-u.ac.jp

Relationship between averaged O-H covalent bond lengths and total energies in supercells

As mentioned in the main manuscript, a hydrogen atom forms a covalent bond with the nearest oxygen atom and a hydrogen bond with the second-nearest oxygen atom. A shorter hydrogen bond length indicates a stronger hydrogen bond. However, attention must be given to the energetics of a 'strong' hydrogen bond.

Fig. S1 shows the relationships between the averaged O-H covalent bond lengths ($\langle d_{O\text{-}H} \rangle$) and the total energies in the 3×3×3 supercells for various compositions. The total energies for each composition are represented by deviations (ΔE) per hydrogen atom from the average energy of the supercells with that composition. When hydrogen bonds form in a supercell, the total energy of the supercell must decrease compared to a hypothetical case where they do not form. Nevertheless, in BSY15H and BSMH with higher dopant concentrations, the total energy appears independent of the average covalent bond length. Supercells with many strong hydrogen bonds are not necessarily more stable than other supercells for a given composition. This is possibly because the formation of many strong hydrogen bonds in a supercell is accompanied by considerable disorder in the atomic arrangement throughout the supercell, making other atomic interactions less effective.

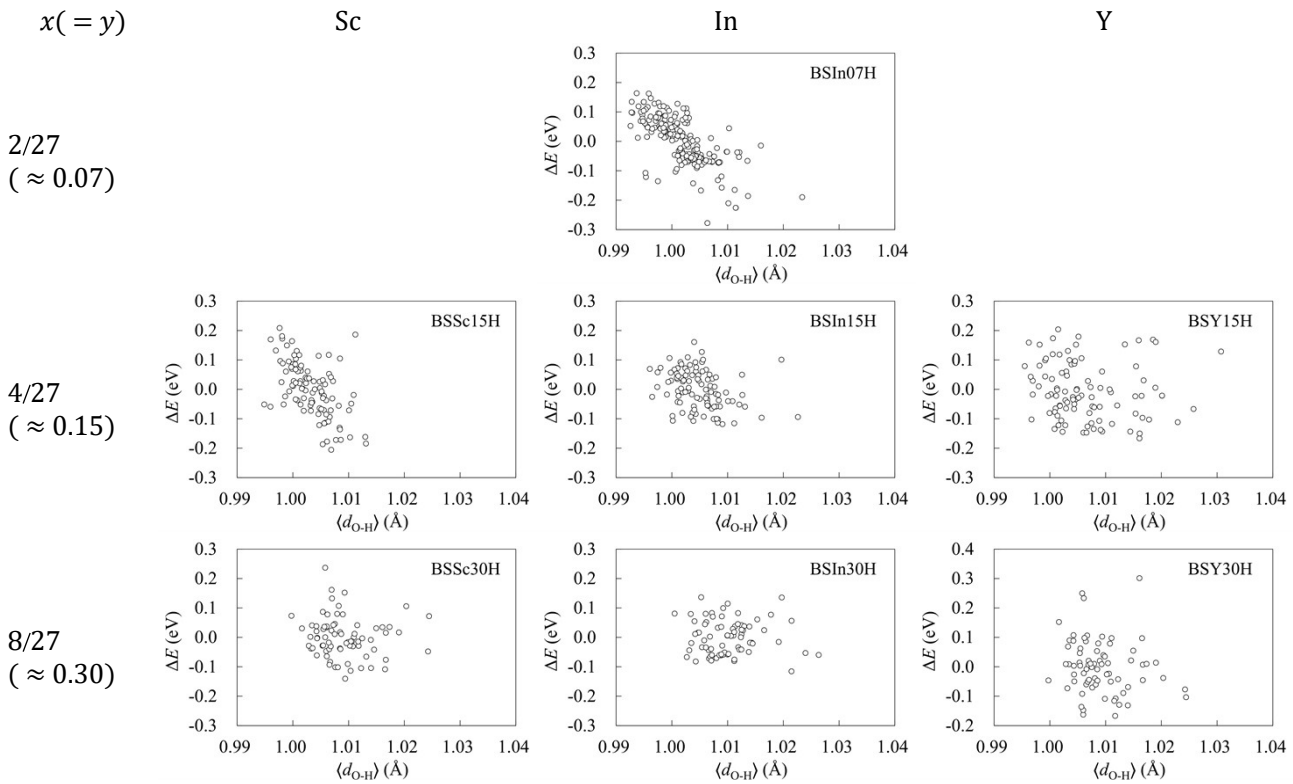

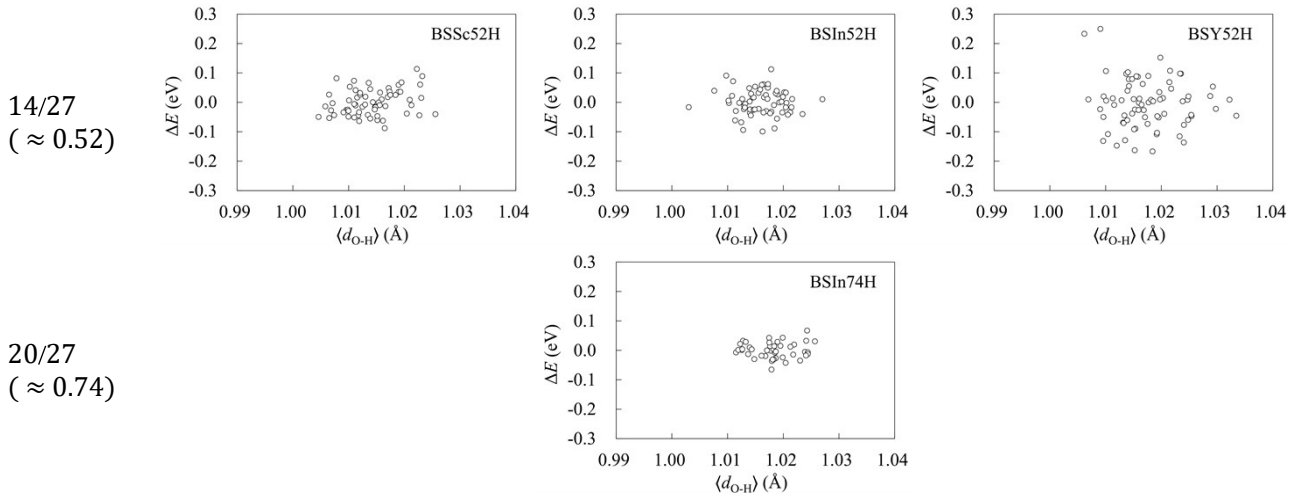

Fig. S1 Relationship between averaged O-H covalent bond lengths and total energies in 3×3×3 supercells for different compositions. Total energies for each composition are represented by deviations (ΔE) per hydrogen atom from the average energy of the supercells with that composition.

Effect of the difference in pseudopotentials

As noted in Section 3.4.1 of the main manuscript, a nearly linear correlation between the O-H covalent bond length and the O-H stretching wavenumber was observed in both the simulation by Balan *et al.*[1-5] and ours. However, the specific linear correlation lines (or curves) did not coincide. To explore the cause of this discrepancy, we performed structural optimization and phonon calculations for BSIn25H and BSIn50H using the same hydrogen pseudopotential that Balan *et al.* used (the scalar-relativistic version included in the SG15 optimized norm-conserving Vanderbilt (ONCV) pseudopotentials[6,7]). The pseudopotentials for elements other than hydrogen, as well as the initial structures, remained unchanged.

Fig. S2(a) illustrates the O-H stretching wavenumber ($\tilde{\nu}$) as a function of the O-H covalent bond length ($d_{O\text{-}H}$). The red symbols represent the same data as plotted in Fig. 18(a) of the main manuscript, which were obtained using the GBRV pseudopotentials for all the atoms in BSInH. The blue symbols represent the data obtained using the SG15 pseudopotential for hydrogen atoms, in combination with the GBRV pseudopotentials for other atoms. The SG15(+GBRV) data, as a whole, shift diagonally towards shorter bond lengths and higher wavenumbers compared to the GBRV data. Additionally, the structures optimized using the different pseudopotentials were sometimes clearly different from each other despite the fact that the initial structures were identical. Specifically, hydrogen atoms sometimes formed covalent bonds and/or hydrogen bonds with different oxygen atoms. On the other hand, the SG15(+GBRV) data for BSInH align well with the data for quartz, corundum, diopside, and dravite as reported by Balan *et al.*[2-5] This result strongly suggests that the discrepancy between Balan *et al.*'s data[2-5] and our GBRV data is not attributable to the differences in substances or calculation methods, but rather to the difference in the hydrogen pseudopotential.

Fig. S2(b) illustrates the integrated molar infrared absorption coefficient (K_{int} in decadic units) as a function of the O-H stretching wavenumber. The red symbols represent the GBRV data, while the blue symbols represent the SG15(+GBRV) data for BSInH. Given the significant scatter in the data, no clear distinction can be observed between the two sets of data. However, both data sets are significantly lower than the SG15 data for quartz,[2] diopside,[4] and tens of minerals[1] as determined by Balan *et al.* (The dash-dotted line represents the calibration proposed by Balan *et al.*[1] for tens of minerals, while the broken line represents the calibration proposed by Libowitzky *et al.* based on experimental data for 10 minerals.[8])

Fig. S2(c) illustrates the O-H stretching wavenumber as a function of the O⋯H hydrogen bond length ($d_{O\cdots H}$). The GBRV data for BSInH are more consistent with the calibration proposed by Libowitzky[8] than the SG15(+GBRV) data for BSInH are. In any case, the variation in pseudopotentials could result in non-negligible differences in infrared absorption spectra. Further investigation into this effect is currently in progress.

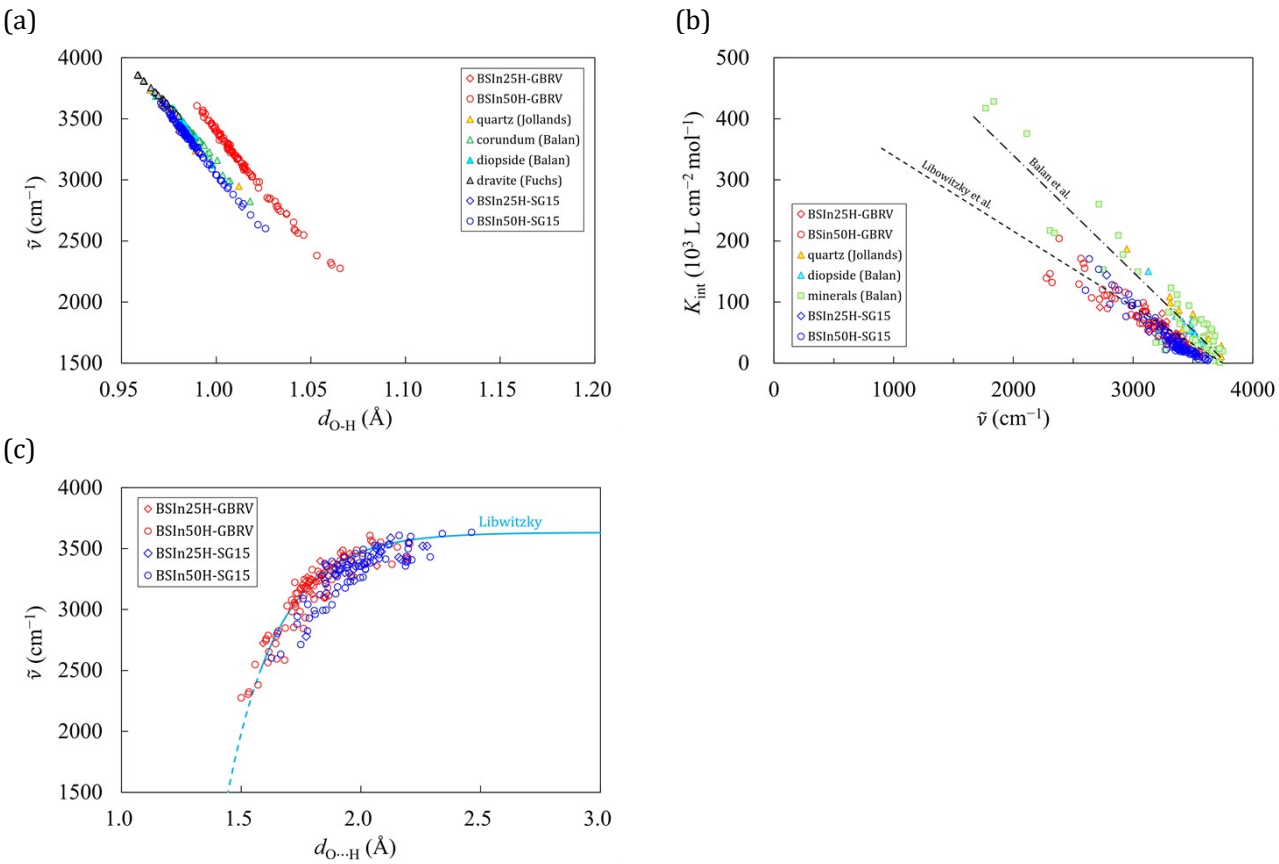

Fig. S2 Comparison between calculation results using the GBRV and SG15 pseudopotentials for hydrogen; (a) O-H stretching wavenumber ($\tilde{\nu}$) as a function of O-H covalent bond length ($d_{O\text{-}H}$), (b) infrared absorption coefficient (K_{int}) as a function of O-H stretching wavenumber, and (c) O-H stretching wavenumber as a function of O⋯H hydrogen bond length ($d_{O\cdots H}$).

References

1 E. Balan, K. Refson, M. Blanchard, S. Delattre, M. Lazzeri, J. Ingrin, F. Mauri, K. Wright and B. Winkler, *Am. Mineral.*, 2008, **93**, 950–953.
2 M. C. Jollands, M. Blanchard and E. Balan, *Eur. J. Mineral.*, 2020, **32**, 311-323.
3 E. Balan, *Eur. J. Mineral.*, 2020, **32**, 457-467.
4 E. Balan, L. Paulatto, J. Liu and J. Ingrin, *Eur. J. Mineral.*, 2020, **32**, 505-520.
5 Y. Fuchs, C. Fourdrin and E. Balan, *Eur. J. Mineral.*, 2022, **34**, 239-251.
6 D. R. Hamann, *Phys. Rev. B*, 2013, **88**, 085117.
7 M. Schlipf and F. Gygi, *Comput. Phys. Commun.*, 2015, **196**, 36-44.
8 E. Libowitzky and G. R. Rossman, *Am. Mineral.*, 1997, **82**, 1111-1115.